Cellulose (2018) 25:4941–4954
https://doi.org/10.1007/s10570-018-1912-2

ORIGINAL PAPER

Chromophores in cellulosics, XVIII. Degradation of the cellulosic key chromophore 5,8-dihydroxy-[1,4]-naphthoquinone under conditions of chlorine dioxide pulp bleaching: a combined experimental and theoretical study

Takashi Hosoya · Nele Sophie Zwirchmayr · Karl Michael Klinger · Heidemarie Reiter · Martin Spitzbart · Thomas Dietz · Klaus Eibinger · Wolfgang Kreiner · Arnulf Kai Mahler · Heribert Winter · Thomas Röder · Antje Potthast · Thomas Elder · Thomas Rosenau

Received: 12 March 2018 / Accepted: 18 June 2018 / Published online: 4 July 2018

Abstract 5,8-Dihydroxy-[1,4]-naphthoquinone (DHNQ) is one of the key chromophores occurring in all types of aged cellulosics. This study investigates the degradation of DHNQ by chlorine dioxide at moderately acidic (pH 3) conditions, corresponding to the conditions of industrial bleaching ("D stage"). The degradation involves three major pathways. As initial reaction, a hydrogen transfer from DHNQ to chlorine dioxide via a PCET mechanism occurs to form a radical $DHNQ^{\cdot}$ and chlorous acid. $DHNQ^{\cdot}$ is then attacked by water to give a pentahydroxynaphthalene radical $PHN^{\cdot}$ that is stabilized by strong delocalization of the non-paired electron into its aromatic ring. $PHN^{\cdot}$ immediately disproportionates to give the observable intermediate 1,2,4,5,8-pentahydroxynapththalene (**I**), which was comprehensively confirmed by NMR and MS (path A). In the presence of excess ClO_2, **I** is immediately further oxidized into acetic acid, glycolic acid, oxalic acid and CO_2 as the final, stable, and non-colored products (path C). In the absence of excess ClO_2, elimination of water from **I** regenerates DHNQ (path B), so that at roughly equimolar DHNQ/ClO_2 ratios ClO_2 is fully consumed while a major part of DHNQ is recovered. To avoid such DHNQ "recycling" under ClO_2 consumption—and to completely degrade DHNQ to colorless degradation products instead—ClO_2 must be applied in at least fivefold molar excess relative to DHNQ.

T. Hosoya
Graduate School of Life and Environmental Sciences, Kyoto Prefectural University, Shimogamo-hangi-cho 11-5, Sakyo-ku, Kyoto-shi, Kyoto, Japan

N. S. Zwirchmayr · K. M. Klinger · A. Potthast · T. Rosenau (✉)
Division of Chemistry of Renewable Resources, Department of Chemistry, University of Natural Resources and Life Sciences, Muthgasse 18, 1190 Vienna, Austria
e-mail: thomas.rosenau@boku.ac.at

H. Reiter · M. Spitzbart
Mondi Uncoated Fine & Kraft Paper GmbH, Marxergasse 4A, 1030 Vienna, Austria

T. Dietz
Evonik-Degussa, Rodenbacher Chaussee 4, 63457 Hanau-Wolfgang, Germany

K. Eibinger
Zellstoff Pöls AG, Dr. Luigi-Angeli-Str. 9, 8761 Pöls, Austria

W. Kreiner · A. K. Mahler · H. Winter
SAPPI Papier Holding GmbH, Brucker Str. 21, 8101 Gratkorn, Austria

T. Röder
Lenzing AG, Werkstraße 2, 4860 Lenzing, Austria

Graphical Abstract

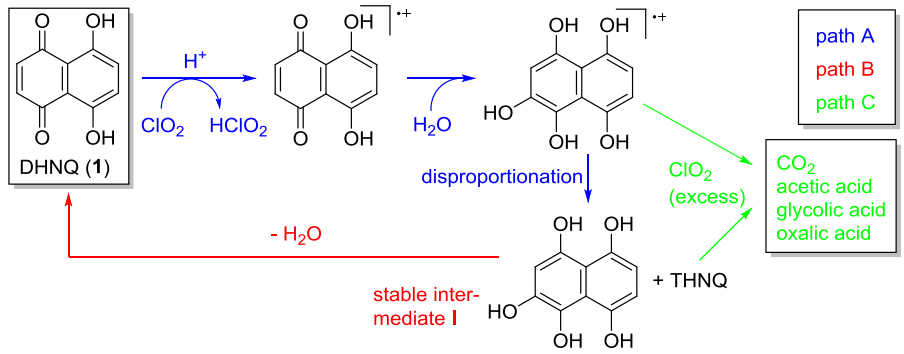

Keywords Cellulose · Pulp bleaching · Chromophores · Brightness · Brightness reversion · Yellowing · 5,8-dihydroxy-[1,4]-naphthoquinone · Chlorine dioxide · Ab initio calculations · Density functional theory (DFT)

Introduction

5,8-Dihydroxy-1,4-naphthoquinone (DHNQ) was reported to be one of the three key chromophores that chiefly contribute to discoloration, often called "yellowing" or "brightness reversion", of cellulosic materials, such as pulp, paper, and fibers (Korntner et al. 2015). The compound is a nearly ubiquitous cellulosic chromophore as it is both a prime survivor of bleaching treatments and a regeneration product from condensation of low-molecular weight fragments upon cellulose aging (Rosenau et al. 2004, 2007, 2008). The high stability of DHNQ toward bleaching treatments is attributed to the exceptional resonance stabilization of DHNQ (Korntner et al. 2015). The double bonds in the peculiar aromatic-quinoid system of DHNQ are much more stable (under both acidic and alkaline conditions) than usual double bonds conjugated with carbonyls: in acidic media, protonated DHNQ, DHNQ-H^+ in Scheme 1, is stabilized because of the conjugation of the positive charge into the aromatic ring, by which the cation becomes less prone toward nucleophilic attacks. In alkaline media, DHNQ is deprotonated to form an exceptionally stable, aromatic dianion (Scheme 1). Considering that most bleaching agents act on localized double bonds, the special stable nature of DHNQ—which lacks such "proper" double bonds due to its canonic forms—and its "survivor qualities" in pulp bleaching become understandable.

The pulp and paper industries are interested in faster and cheaper removal of the compound from cellulosic pulps, and in minimizing its re-formation. Fast and reliable methods to detect and quantify DHNQ at very low concentrations—normally in the low ppm to ppb range in cellulosic pulps—have become available (Potthast et al. 2018), which is a prerequisite to monitoring bleaching attempts. Several previous accounts have addressed the chemistry of DHNQ which has recently been reviewed (Hosoya et al. 2013). Its main reaction paths are cycloaddition to the 2,3-double bond with various dienes (Lanari et al. 2002; Cuellar et al. 2003; Tandon et al. 2005), nucleophilic addition mainly at the 2-position (Arnone et al. 2007; Zhou et al. 2009; Tandon et al. 2004, 2005, 2009, 2010; Valderrama et al. 2003; Greco et al. 2010), and derivatization of the hydroxyl groups (Betts et al. 2004; Mital et al. 2008; Kelly et al. 2000). While these works focused on DHNQ as a synthon or as an analytical target molecule, its revival, which is linked to its recently recognized central role in cellulose yellowing, put especially its degradation chemistry and "discoloration" in the focus of studies (Zwirchmayr et al. 2017).

T. Elder
USDA Forest Service, Southern Research Station, 521 Devall Dr, Auburn, AL 36849, USA

T. Rosenau
Johan Gadolin Process Chemistry Centre, Åbo Akademi University, Porthansgatan 3, 20500 Åbo/Turku, Finland

Environmental implications and concerns notwithstanding, chlorine dioxide-based pulp bleaching, called D-stage bleaching, is still one of the most frequently utilized bleaching approaches for cellulosic pulps on industrial scale. Chlorine dioxide is a strong oxidant for variety of organic compounds, such as phenols, aldehydes, unsaturated structures, or amines. It undergoes hydrogen atom abstraction, one-electron transfer, and radical addition reactions to double bonds (Leigh et al. 2014; Aguilar et al. 2014; Lehtimaa et al. 2010; Napolitano et al. 2005; Hull et al. 1967). It is a favored oxidant in pulp bleaching because of its high selectivity, meaning that residual lignin, with its aromatic and quinoid structures, is attacked while the carbohydrate structures of cellulose and hemicelluloses remain largely unharmed. This is one advantage over oxygen-based bleaching chemicals, such as molecular oxygen (O-stage bleaching), hydrogen peroxide (P-stage) or ozone (Z-stage), which are less selective, but trump with regard to environmental benignity. Giving the profound role of DHNQ in discoloration of cellulosics, the mechanisms in degradation of DHNQ by chlorine dioxide is one of the central reactions in production of highly bleached pulps. This study addresses the molecular mechanisms of the degradation of DHNQ by chlorine dioxide, based on experimental results which are then correlated with computational insights.

Results and discussion

Experimental studies

Chlorine dioxide has a doublet ground state. It is a thus radical with its spin being delocalized mainly between the two oxygen atoms, with only minor contributions of spin density at the central chlorine atom. The Cl has the formal oxidation state of IV, which is rather unstable and accounts for the compound´s high reactivity (Scheme 1). Due to its complex redox chemistry and the superposition of disproportionations and symproportionations between derived chlorine-oxygen species [chloric acid (V), chlorous acid (III), chlorine (0), hypochlorous acid (1), chloride (− 1)] in aqueous solution, it is impossible to record reaction kinetics following ClO_2 itself, so kinetic monitoring must rely on following the (organic) coreactant. Similarly, because of the very presence of reactive chlorine-oxygen species, it is hard to decide whether oxidation of a compound was effected by ClO_2 itself, by one of its derived secondary oxidants, or by a mixture of those.

We first attempted to evaluate the rate of DHNQ degradation by chlorine dioxide through the time dependency of the visible spectrum of the reaction solution, see Fig. 1 for a solution of DHNQ (21.9 µmol/L) at pH 3. The spectrum showed two peaks at 515 and 489 nm along with a shoulder at 550 nm. When chlorine dioxide was added to the solution, its prominent peak around 355 appeared. To avoid any interference and overlapping with the DHNQ peaks at 515 and 489 nm, we followed the DHNQ degradation on the basis of the shoulder peak at 550 nm, which is far enough separated from that of ClO_2.

A degradation experiment at pH 3 with an 1:1 molar ratio between DHNQ and chlorine dioxide showed the absorbance at 550 nm to decrease in the initial 420 s and then to start rising again at a slow rate. To get further information, we performed a larger-scale experiment (see experimental section for the detailed procedures) with DHNQ/ClO_2 starting ratios of 1:1 and 1:2. Titration of the reaction solution (see experimental section for details) confirmed that in both cases no chlorine dioxide was left after 420 s (the absence being reconfirmed after 30 min and 2 h). The reaction was followed directly by ^{1}H NMR (water signal suppression), using an aliquot of the reaction mixture. In addition, aliquots of the aqueous reaction solution were taken at different time intervals, extracted with chloroform and analyzed by NMR and GC–MS. After a reaction time of 420 s, 74% of the DHNQ had been consumed in the case of a 1:1 starting ratio (26% were left unchanged), but nevertheless 85.2% of the starting DHNQ was recovered after a reaction time of 2 h (see Fig. 3). NMR indicated the presence of an intermediate (see below), which had its maximum concentration (22% of starting DHNQ) after 7–10 min, and was constantly decreasing until it became undetectable after about 70 min. This evidently pointed to a fast initial consumption of DHNQ and conversion into an intermediate, which was followed by a slow re-

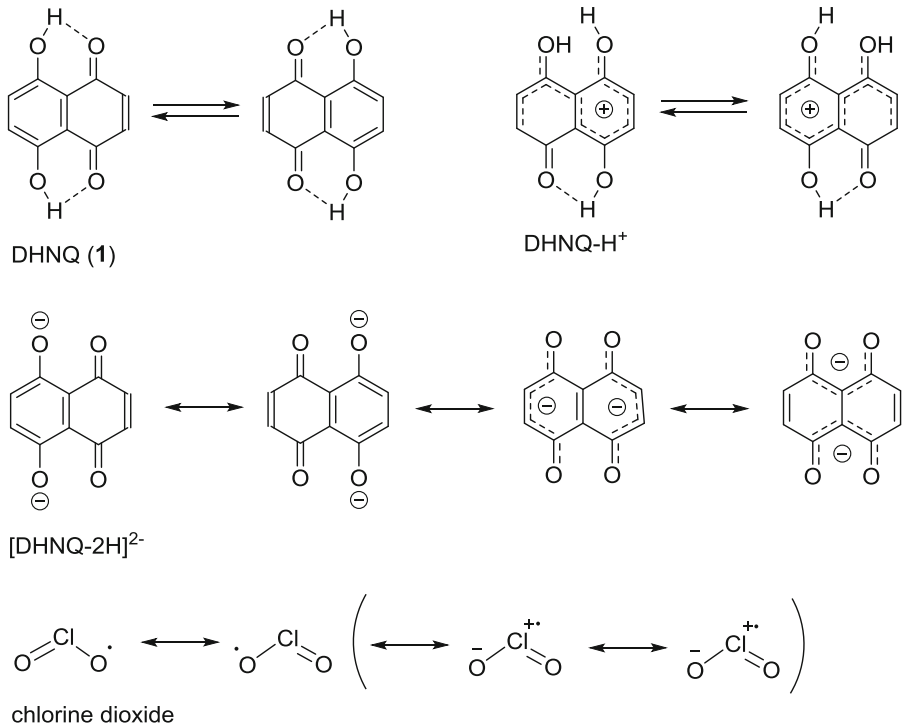

Scheme 1 Chemical structures of DHNQ (**1**) and its protonated and deprotonated forms, DHNQ-H^+ and $[DHNQ\text{-}2H]^{2-}$, respectively, along with the structure of chlorine dioxide

formation of DHNQ under consumption of this intermediate.

The situation changed for a DHNQ/ClO_2 starting ratio of 1:2, i.e. the double molar amount of ClO_2. After 420 s, only 15% of starting DHNQ was left, after about 15 min it was completely consumed, and only 8% was regenerated after 2 h, this value not further increasing with extended reaction times (10 h). The intermediate was detected only shortly, between 2 and 6 min reaction time, in rather low concentrations, with a maximum of 6% rel. to starting DHNQ at 3–4 min.

The above results suggested a mechanism as shown in Scheme 2. DHNQ reacts with chlorine dioxide to form an intermediate **I** (path A), which must be colorless or at least have much less intensive color than DHNQ. In the absence of excess ClO_2, the intermediate slowly reacts back to DHNQ (path B). This pathway B cannot be simply the reverse process of path A, since no re-formation of chlorine dioxide was observed after 420 s up to 2 h. As to the stoichiometry of path A, it would be reasonable to assume that chlorine dioxide converts one molar equivalent of DHNQ to **I**, although only around three quarters of the initial DHNQ had been consumed at 420 s. This incomplete conversion of DHNQ at 420 s is explained by the (many) side reactions of ClO_2, i.e. by incomplete consumption, by path B setting in, i.e. regeneration of DHNQ, and by consumption of chlorine dioxide in the slower reaction with intermediate **I** (path C), i.e. consumption of the coreactant by parallel processes. The latter process is irreversible and eventually converts DHNQ—via **I**—into the final degradation products, namely carboxylic acids and CO_2 (Scheme 2).

At low ClO_2 concentrations, for instance at the initially used molar ratio of 1:1 between DHNQ and ClO_2, the path B dominates, but with increasing DHNQ/ClO_2 ratios, path C becomes increasingly dominant. This is supported by the fact that at a 1:1 DHNQ/ClO_2 ratio there is an initial consumption of 74% DHNQ after 5 min, and a final regeneration of 67% DHNQ after 2 h. When ClO_2 was used substoichiometrically (DHNQ/ClO_2 2:1), nearly the theoretical amount of DHNQ was consumed initially (44%), and 72% of DHNQ was recovered after 2 h. At a 1:2 ratio, 98% of DHNQ was consumed after 5 min,

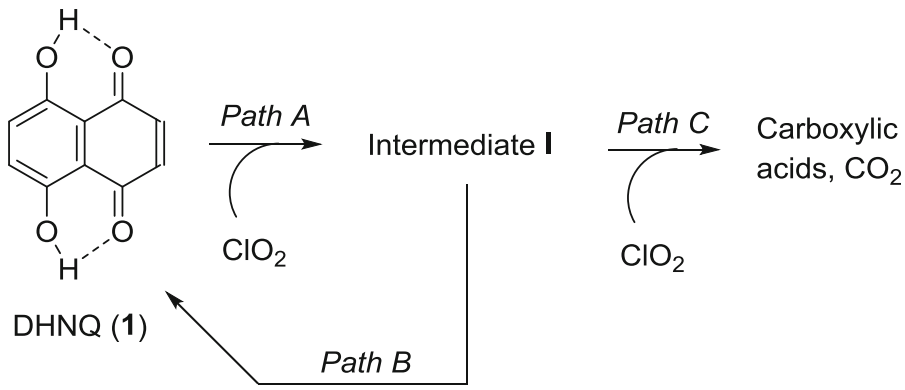

Scheme 2 General mechanism of the DHNQ reaction with chlorine dioxide

and only 12% was finally re-formed after 2 h. At a 1:3 ratio, DHNQ was completely consumed after 5 min, and only traces (< 0.2%) of regenerated DHNQ was detectable after 2 h. At larger ClO_2 excess (ratio DHNQ/ClO_2 5 or above), no DHNQ was recovered at all, nor was **I** or any other intermediate found in detectable concentrations (VIS, NMR): the reaction went "straight through" to the final reaction degradation products.

When the degradation reaction at a 1:1 ratio was performed with addition of D_2O, replacing 2/3 of the initially used H_2O, the rates of paths A and B were significantly lowered (Fig. 2). Evidently, water is directly involved as a reactant in the process and not just as a solvent and reaction medium, so that kinetic isotope effects (H–D) come into play. This can be the case for keto-enol tautomerisms (H^+ shifts), additions or eliminations (HO^-/DO^-), or hydrogen atom ($H^{\cdot}$) abstraction reactions, which all would be influenced by H/D differences. Especially the last alternative seemed tempting, because in radical H abstraction reactions, deuterium transfer is usually significantly slower than hydrogen transfer (while the effect on tautomerisms or simple H–D exchange in hydroxyl groups is minor)—which in turn would agree with the observed, relatively strong effect. This issue will be discussed with the computational results in the next section.

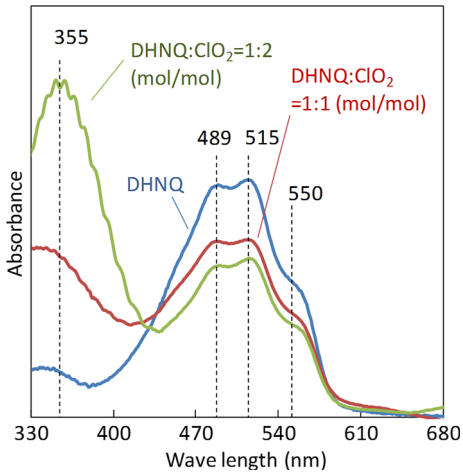

Fig. 1 Visible spectra of an aqueous DHNQ solutions (0.1 mM, pH = 3) with or without aqueous chlorine dioxide added. Spectra were recorded within 10 s after ClO_2 addition

Figure 3a shows the TLC analysis of a chloroform extract of the 1:1 (molar ratio DHNQ/ClO_2) reaction after 5 min, obtained by fast shaking of 1 ml of aqueous reaction mixture with the same amount of $CDCl_3$ and immediate TLC analysis or immediate transfer into the NMR spectrometer. The extract contained two main components: the deeply colored starting material DHNQ and intermediate **1** as a more polar compound having no VIS absorption, but a distinct absorption in the UV region at 254 nm. Besides the dominant solvent and DHNQ signals, the ^1H NMR spectrum exhibited two doublets and a singlet in the aromatic region, evidently coming from intermediate **I** (Fig. 3b): these resonances disappeared within 3 min in the case of the crude extract, leaving only the DHNQ signal behind. Since no other peaks appeared instead, it was conclusive that this second, transient compound degraded into DHNQ. When the crude $CDCl_3$ extract was filtered through a layer of solid $MgSO_4$ and K_2CO_3 before the NMR measurement to remove traces of water and acids, the resonances of the second component remained

observable for about 2 h before they vanished, once more leaving behind DHNQ as the only observable component. Trimethylsilylation (TMS) in the NMR tube by an excess of *N,O*-bis(trimethylsilyl)-trifluoroacetamide (BSTFA) had no significant effect on the ^{1}H chemical shifts of **I** ($\Delta\nu < 0.04$ ppm), but considerably increased the stability of the compound, which in the TMS-derivatized form seemed to be almost indefinitely stable, with no apparent loss in signal intensity even after 14 days. The presence of five trimethylsilyloxy resonances indicated that intermediate **I** carried five OH groups which by reaction with BSTFA had apparently been converted into their TMS-derivatives.

Unambiguous proof of the nature of intermediate **I** was provided by DESI-MS analysis (Schedl et al. 2016) from both the TLC plate and in the paperspray-MS setup (Potthast et al. 2018; Wenger et al. 2015; Schedl et al. 2017). The compound was identified as 1,2,4,5,8-pentahydroxynaththalene, the mass data of the compound and its penta(trimethylsilyl) derivative being presented in Table 1. The TMS-derivative **I-TMS** contained the five TMS-protected OH groups that were already assumed from ^{1}H NMR. Compound **I** can be conceived as a formal addition product of water to DHNQ: water is added to the quinoid double bond in DHNQ, followed by conversion of the two keto groups into their enolic counterparts, which means rearomatization to a naphthalene system. However, it should be well noted that this is just a mnemonic to visualize the interrelation between the two compounds—the process of water addition to DHNQ to form **I** does not proceed in reality, and aqueous solutions of DHNQ are completely stable, independent of the pH. The observed formation of **I** from DHNQ in the reaction system thus must be due to the presence and action of ClO_2, and cannot be a direct water addition process.

However, the reverse process, i.e. elimination of water from **I** to give DHNQ, is obviously a spontaneous process. It was observed both in aqueous medium upon the bleaching experiments (UV) and also in the organic medium of the chloroform extracts (NMR). The facile conversion from **I** back to DHNQ can also nicely be visualized by TLC. The VIS-innocent spot of **I** (see Fig. 3a) turned—with slowly increasing intensity—into the bluish color of DHNQ within 30 min under ambient conditions. The conversion became immediate when the TLC plate was exposed to vapor of hydrochloric acid or trifluoroacetic acid, or when sprayed with these acids. Interestingly, exposition to ammonia vapor or spraying with dilute NaOH had a similar accelerating effect, also causing immediate appearance of a visible color, the dark blue hue of the DHNQ dianion. While in general acidic media facilitate elimination of water by protonation of the reacting hydroxyl groups, in alkaline media the formation of the highly stabilized DHNQ-dianion must be assumed as the driving force.

As described above, at a DHNQ/ClO_2 ratio of 1:5, no intermediate **I** was detected and thus no DHNQ was re-formed from it. The reaction mixture contained small gas bubbles adhering to the walls of the reaction vessel, which were identified as CO_2 both directly by purging the gas into an aqueous $BaCl_2$ solution, which formed a white precipitate. The precipitate was soluble in dilute (2 N) HNO_3 under evolution of a gas. Also, the reaction mixture was brought to pH 10 by 2 N NaOH. ^{13}C NMR showed a prominent carbonate peak, and addition of aqueous $Ba(OH)_2$ gave a HNO_3-soluble precipitate. All these results point to CO_2 being one of the main final reaction products. GCMS analysis of the reaction mixture after extraction according to a protocol optimized for mixtures of acids and hydroxyacids in complex matrices (Liftinger et al. 2015) showed the three acids acetic acid, glycolic acid and oxalic acid in an approximate ratio of 1:1.2:6.2. The result of quantitative ^{13}C NMR was in very good agreement (1:1.2:6.8). The degradation of DHNQ was complete within less than 30 min: the NMR and GCMS results

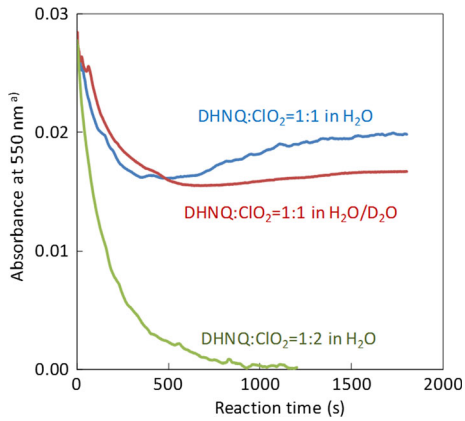

Fig. 2 Time course of the degradation of DHNQ by ClO_2 (pH 3, 0.03 mM), seen by VIS absorbance at 550 nm. In the H_2O/D_2O experiment, 66% of H_2O was replaced with D_2O

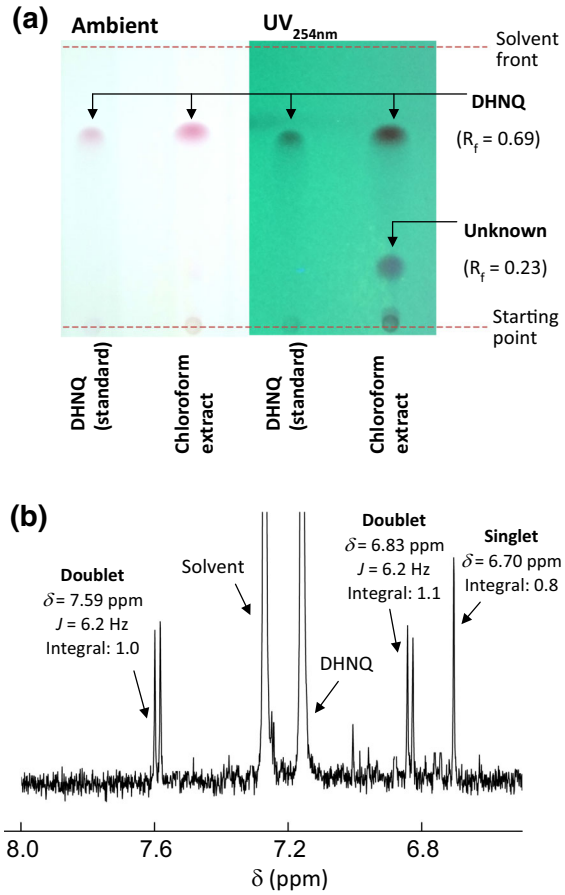

Fig. 3 Reaction of DHNQ and chlorine dioxide (molar ratio 1:1), reaction mixture after a reaction time of 5 min. **a** TLC analysis of the crude chloroform ($CDCl_3$) extract, eluant: ethyl acetate/*n*-heptane (v/v = 1:1). **b** ^{1}H NMR spectrum of the chloroform extract ($CDCl_3$) after filtration through a layer of solid $MgSO_4$ and K_2CO_3. Note that the four C–H protons of DHNQ appear as singlet due to quick intramolecular proton transfers, solvent peak (trace $CHCl_3$) at 7.26 ppm

after 30 min, 2 h, and 5 h reaction time were identical. The ratio between the three acids seemed to be very well reproducible (three independent runs) and largely constant at a fixed DHNQ/ClO_2 ratio, with acetic acid and glycolic acid being formed in roughly equimolar ratio, and oxalic acid in about the fivefold molar amount. The sum of these three organic acids accounted for 42% of the carbon atoms in the starting DHNQ, the rest being converted into CO_2.

Computational studies

The initial steps in the reaction between DHNQ and ClO_2 were computationally evaluated on the CCSD(T)/BS-II and DFT(M06-2X)/BS-II levels of theory, suggesting the detailed mechanism shown in Scheme 3. The first step of path A is a hydrogen atom transfer from protonated DHNQ starting material (DHNQ-H^+) to chlorine dioxide, which results in formation of a radical cation DHNQ$^{\cdot+}$ and chlorous acid, $HClO_2$. This reaction proceeds according to a proton-coupled electron transfer (PCET) mechanism (Schedl et al. 2017), as shown in the potential energy curve in Fig. 4. The proton from the quinone oxygen of DHNQ-H^+ is transferred to the ClO_2 coreactant which is in the doublet (radical) state, followed by a state jump (i.e. electron transfer), by which the DHNQ part becomes the radical while non-radical $HClO_2$ is formed. This PCET reaction is also supported by the experimental result that the degradation was retarded in the presence of D_2O (Fig. 2).

The geometry of the state jump (SJ) was determined from the potential energy curve in Fig. 4. Evaluation at the DFT(M06-2X) level (with the larger basis set BS-II, see computational section) afforded a potential energy of 24.6 kcal/mol relative to the starting DHNQ. This energy can be only used as a rough estimate of the activation energy (E_a) of the PCET reaction; it is overestimated (too positive, usually by 10–15%), since effects of resonance interaction between the states 1 and 2 and tunneling of the hydrogen are not taken into account (Tishchenko et al. 2008). As an in-depth evaluation of these effects would not add anything substantial to the understanding of the mechanism, we did not make further efforts to optimize the energy computations of the SJ state. More importantly, the activation energy became significantly higher (30.1 kcal/mol) when the PCET reaction started from non-protonated DHNQ. This strongly suggested that the formation of DHNQ-H^+ is a prerequisite to the PCET reaction. In fact, it was experimentally observed that the degradation became much slower when the pH of the reaction solution was increased from 3 to 6, which confirms this computational prediction.

After the PCET reaction, two molecules of chlorous acid disproportionate into the more stable hypochlorous acid HClO and chloric acid $HClO_3$ (Hull et al. 1967). The Gibbs energy of the radical cation

Table 1 MS data of 1,2,4,5,8-pentahydroxynaththalene (PHN, I) and its penta(trimethylsilyl) derivative (**I-TMS**)

	PHN (intermediate **I**)	Derivative **I-TMS**
chemical formula	$C_{10}H_8O_5$	$C_{25}H_{48}O_5Si_5$
molecular weight	208.17	569.07
exact mass, cald.	208.3717	568.2348
exact mass $[M + H]^+$, calcd.	209.0444	569.2421
exact mass $[M + H]^+$, calcd.	209.0438	569.2430
exact mass $[M - H]^-$, calcd.	207.0299	–
exact mass $[M - H]^-$, calcd.	209.0305	–

$DHNQ^{\cdot+}$ after this disproportionation eventually becomes − 3.5 kcal/mol (Fig. 4), indicating that $DHNQ^{\cdot+}$ is stable enough to render the reverse process of the PCET reaction negligible. $DHNQ^{\cdot+}$ is in equilibrium with its deprotonated form, the neutral DHNQ radical. The above result on the structure of intermediate **I** led us to investigate the process of water addition to $DHNQ^{\cdot+}$, forming a pentahydroxynaphthalene radical cation $PHN^{\cdot+}$ (Scheme 3). The activation barrier in the formation of $PHN^{\cdot+}$ from $DHNQ^{\cdot+}$ was calculated to be quite small, $\Delta G^{0\ddagger}$ = 16.3 kcal/mol relative to $DHNQ^{\cdot+}$, with the resulting $PHN^{\cdot+}$ being much more stable than $DHNQ^{\cdot+}$: the Gibbs energy of $HHN^{\cdot+}$ is − 24.0 kcal/mol relative to $DHNQ^{\cdot+}$. These results indicate that $DHNQ^{\cdot+}$, as soon as formed by reaction between DHNQ and ClO_2, immediately adds water being converted to more stable $PHN^{\cdot+}$. The water addition is only favored in the case of the radical cations, i.e. the protonated species. For the neutral radicals, i.e. the addition of water to $DHNQ^{\cdot}$ giving $PHN^{\cdot}$, the higher activation energy excludes the direct water addition process, which takes the "detour" via the protonated species instead (Scheme 3). The large difference in the stability between $DHNQ^{\cdot+}$ and the more stable $PHN^{\cdot+}$ deserves some consideration, because often symmetric radical species (such as $DHNQ^{\cdot+}$) are more stable than non-symmetric ones (such as $PHN^{\cdot+}$) so that the opposite behavior should be assumed at a first glance. The decisive stability factor is that the radical cation can be easily accommodated, i.e. delocalized and stabilized, in the relatively large, aromatic naphthalene system whereas stabilization is much harder in the half-quinoid DHNQ.

Computation at the CCSD(T)/BS-II level indicated that the $PHN^{\cdot+}$ radicals very easily undergo disproportionation leading to one molecule of PHN (intermediate **I**), its corresponding quinone THNQ and two protons (Scheme 3). Intermediate **I** is then readily reconverted into DHNQ by release of water (Scheme 4). The MP4(SDQ)/BS-III method was employed instead of the CCSD(T)/BS-II method, as the MP4(SDQ) calculations with a bigger basis sets (BS-III) are more reliable than the CCSD(T) ones with relatively smaller basis sets (BS-II) in these ionic reactions. This entire process corresponds to path B in Scheme 2, the regeneration step of DHNQ. This reaction proceeds only if no excess ClO_2 is present to convert **I** into the final, stable carboxylic acid products. DHNQ is about 2 kcal/mol more stable than **I** on the basis of calculated Gibbs energy. The activation barrier of these conversions is expected to be small, as the processes are essentially a combination of keto-enol interconversions which, in general, occur readily at room temperature.

Two $PHN^{\cdot+}$ radicals form one molecule of **I** by disproportionation which in turn gives back one molecule of DHNQ by water elimination (Schemes 3 and 4). Thus, half the originally consumed stoichiometric amount of DHNQ would be regenerated—once again, this applies only if no excess ClO_2 is present. There was a quite satisfying agreement with the experimentally observed kinetics: At 74% initial consumption, 71% of DHNQ should be regenerated theoretically (26% not consumed initially plus 74/2 = 37% of regenerated DHNQ), while 67% were found experimentally. When 44% DHNQ were consumed initially, 78% of DHNQ (56 + 44/2) should be found after the reaction according to theory, and 72% were indeed detected. The quinoid product of the disproportionation, 2,5,8-trihydroxy-1,4-naphthoquinone (*cf.* Scheme 3), is not stable in aqueous medium as known from previous studies (Zwirchmayr et al. 2017). It undergoes ring contraction of the quinoid part, which removes the special stabilization of the DHNQ system (see Scheme 1) so that the

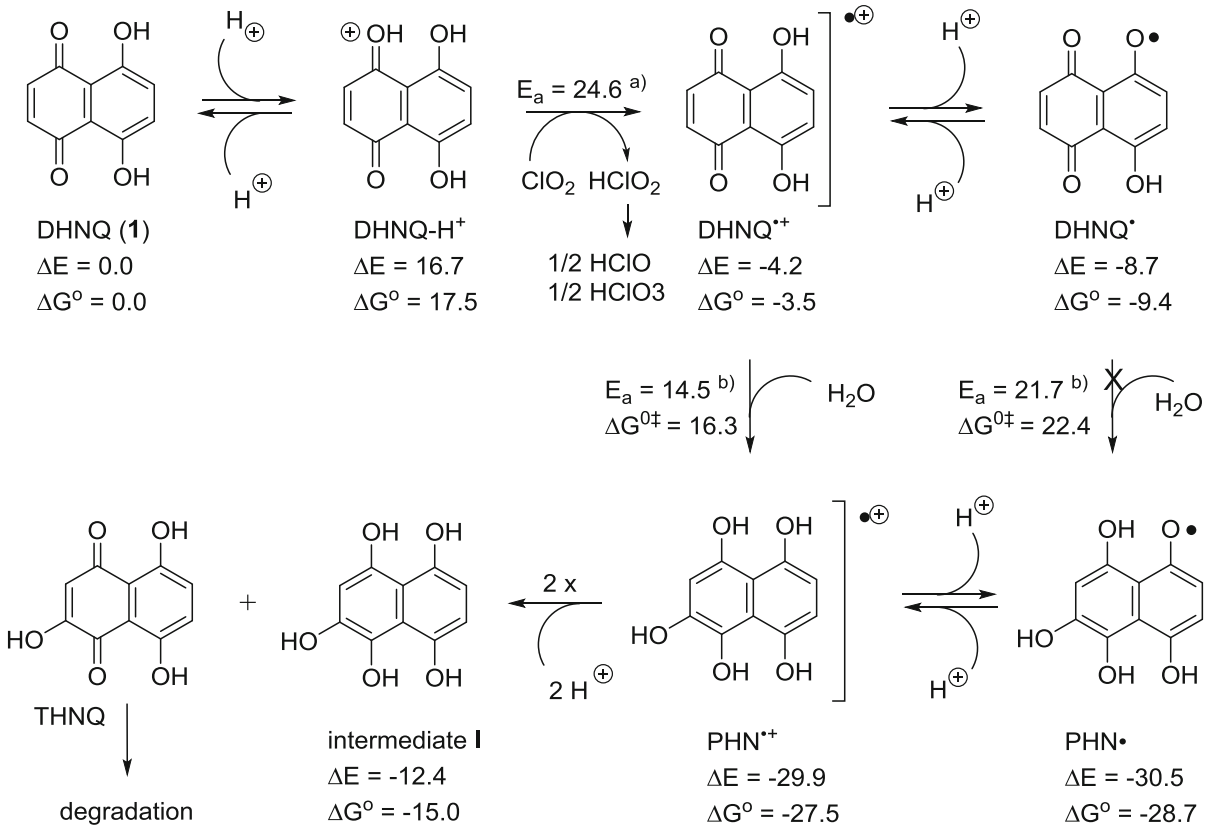

Scheme 3 Mechanism of path A (*cf.* Scheme 2) from computations at the CCSD(T)/BS-II level of theory. Energies are shown in kcal/mol. [a)]The energy of the state jump in the PCET reaction was calculated at the DFT(M06-2X)/BS-II level because the CCSD(T) calculation was not possible, see Fig. 4 for the geometry of the state jump. [b)]The activation barriers for the water addition were evaluated separately at the DFT(M06-2X) level with six explicit solvent (water) molecules taken into consideration

aromatic part, now a rather oxidation-labile hydroquinone structure is fast further converted and degraded to low-molecular weight carboxylic acid products (Zwirchmayr et al. 2017).

It is interesting to compare the relative stabilities between the cation radicals $PHN^{\cdot+}$ and $DHNQ^{\cdot+}$ and the non-radical parent molecules PHN and DHNQ. $PHN^{\cdot}$ is 19.3 kcal/mol more stable than $DHNQ^{\cdot}$ based on Gibbs energy (Scheme 3), while the situation is opposite for the neutral PHN (**I**)/DHNQ pair: DHNQ becomes 1.9 kcal/mol more stable than the corresponding water adduct PHN (Scheme 4). This explains why DHNQ does not add water, while $DHNQ^{+}$ does, and why **I** tends to eliminates water to re-form DHNQ. As mentioned above, the non-paired electron in $PHN^{\cdot+}$ is more delocalized and hence more stabilized than that in $DHNQ^{\cdot+}$. In the non-radical molecules PHN and DHNQ such additional stabilization does not exist. This stability inversion occurring upon going from the radical to the non-radical species is one of the essential driving forces to implement the reaction cycle consisting of the paths A and B (Scheme 2).

Conclusions

Our experimental and theoretical investigations addressed the molecular mechanisms of ClO_2 degradation of DHNQ under conditions of an industrial D bleaching stage. The individual steps in the reaction system can be grouped into three pathways. Pathways A describes the formation of a stable intermediate by reaction of DHNQ and ClO_2, path B the reformation of DHNQ from this intermediate, and path C the formation of stable, low-molecular weight

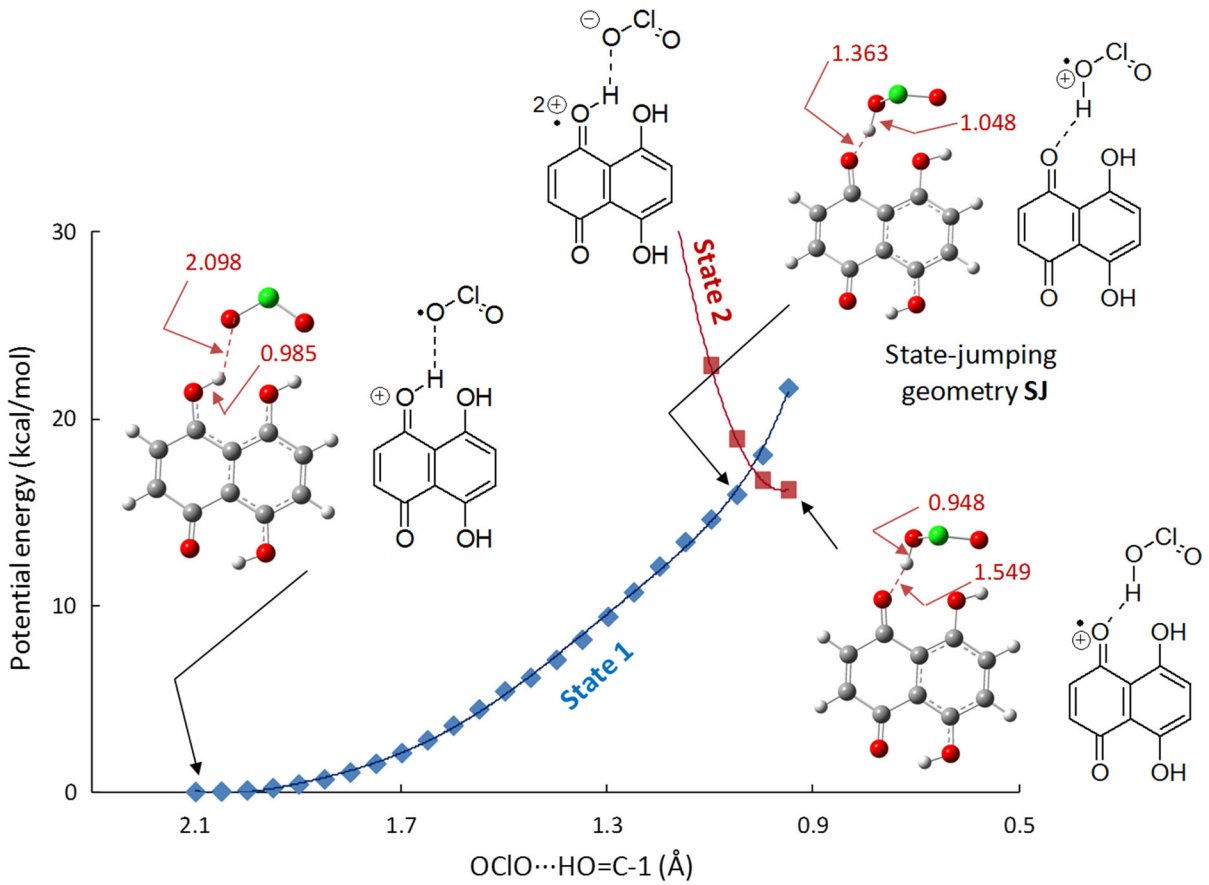

Fig. 4 Potential energy curve of the DHNQ-H^+–ClO_2 complex, calculated at the DFT(M06-2X)/BS-I level of theory, the intersection of the two curves indicating the state jump (SJ). The potential energies are given relative to that of the starting complex, bond lengths are given in Å

degradation products from the intermediate. Path B comes into play if no excess ClO_2 is present, so that pathways A and B together effect a 50% "recycling of DHNQ". Otherwise, with excess ClO_2 oxidant being present, path C is operative.

The hydrogen transfer from protonated DHNQ to ClO_2 according to a PCET mechanism is the initial reaction step. The resulting radical cation $DHNQ^+$ easily adds water to give a pentahydroxy naphthalene radicals $PHN^{\cdot+}$, which readily disproportionate into intermediate 1,2,4,5,8-pentahydroxynaphthalene (PHN, **I**) and trihydroxynaphthoquinone (THNQ). These reactions are contained in path A in Scheme 2. In the absence of chlorine dioxide, **I** eliminates water to regenerate DHNQ (path B). Under usual bleaching conditions, i.e. with excess ClO_2 being available, intermediate **I** and trihydroxynaphthoquinone are degraded according to complex parallel mechanisms into carbon dioxide, acetic acid, glycolic acid and oxalic acid (path C), which all were identified in the reaction mixture. The final products are colorless compounds which (with the exception of gaseous CO_2) are completely soluble under the reaction conditions and readily washed out.

To avoid the "recycling" of DHNQ under consumption of ClO_2, it is imperative that ClO_2 is used in at least fivefold molar excess. While under industrial conditions the net amount of ClO_2 is usually large enough, local concentrations can be insufficient due to limited mixing. Therefore, lower ClO_2 charges bear the danger of inefficient DHNQ removal due to the recycling reaction (paths A and B in combination) setting in at the expense of path C. Another precaution is the use of sufficiently acidic conditions. As the initial step of the reaction requires protonation of DHNQ, pH values above 4.5 should be avoided.

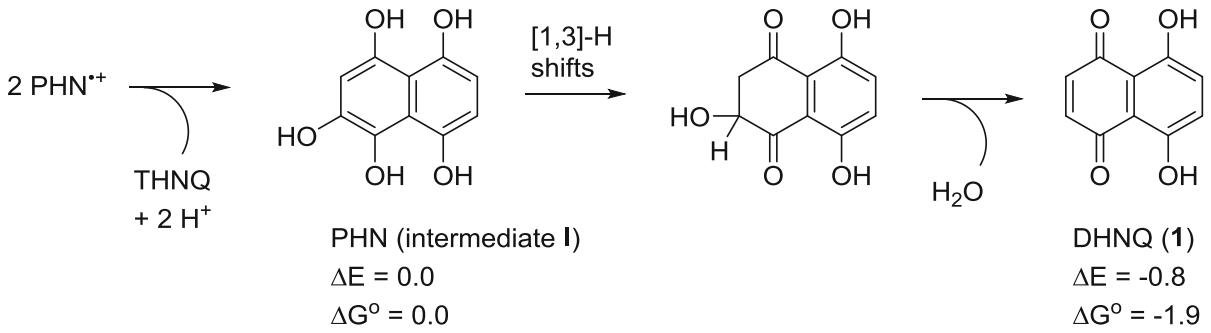

Scheme 4 Mechanism of path B, elimination of water from **I** to regenerate DHNQ (*cf.* Scheme 2) from computations at the at the CCSD(T)/BS-II level. DHNQ is regenerated in half the stoichiometric amount of initially available $PHN^{\bullet+}$ in good agreement with experimental data. Energies are shown in kcal/mol

Otherwise, the consumption of DHNQ becomes too slow, and disproportionation reactions of ClO_2 become dominant.

Experimental

General

Commercial chemicals from Sigma-Aldrich (Schnelldorf, Austria) were of the highest grade available and were used without further purification. Distilled water was used for all aqueous solutions.

For NMR analysis, a Bruker Avance II 400 instrument (^{1}H resonance at 400.13 MHz, ^{13}C resonance at 100.61 MHz) with a 5 mm broadband probe head (BBFO) equipped with z-gradient with standard Bruker pulse programs and temperature unit were used. Data were collected with 32 k data points and apodized with a Gaussian window function (GB = 0.3) prior to Fourier transformation. ^{1}H NMR data were collected with 32 k complex data points and apodized with a Gaussian window function (lb = − 0.3 Hz,gb = 0.3 Hz) prior to Fourier transformation. ^{13}C-jmod spectra with WALTZ16 ^{1}H decoupling were acquired using 64 k data points. Signal-to-noise enhancement was achieved by multiplication of the FID with an exponential window function (lb = 1 Hz). Bruker TopSpin 3.5 (3.0) was used for the acquisition and processing of the NMR data. Chemical shifts are given in ppm, referenced to residual solvent signals (7.26 ppm for ^{1}H, 77.0 ppm for ^{13}C).

An Agilent 6560 QTOF mass spectrometer equipped with an Agilent G1607A dual Jetstream coaxial ESI interface was used, injection volume: 5 µL, sheath gas temperature: 150 °C, sheath gas flow rate: 12 L/min, nebulizer gas pressure: 20 psi, MS capillary voltage: 4 kV, nozzle voltage: 2 kV, fragmentor: 275 V, scanning mass range 50–1700 m/z with a TOF acquisition rate of 2.8 spectra/s.

For paperspray MS, the paper tips (isosceles triangle, a = 10 mm) were cut and connected to 4 kV capillary voltage. Whatman filter paper No 1 (Wagner & Munz GmbH, Vienna, Austria) was used as the model sample matrix. The aqueous sample solution was used as a spray solvent. After applying 30 µL of the spray solvent onto the paper surface, mass spectra were recorded in positive or negative ion mode with a Thermo LTQ-MS (LTQ XL^{TM} Linear Ion Trap Mass Spectrometer, Thermo Fisher Scientific, Waltham, Massachusetts, USA) equipped with an ESI ion source. Injection volume: 5 µL. Where applicable, a splitter with the ratio of 1:2 was used to divert the flow for better ESI spray quality. MS settings: Spray voltage: 6 kV, sheath gas pressure: 5 psi, auxiliary gas: 2 a.u., transfer capillary temperature: 275 °C, scan range: m/z 300–1000. In case of tandem-MS investigations, an isolation width of ± 0.5 m/z was selected. Thermo Fisher Scientific Xcalibur software (Thermo Xcalibur 2.2 SP1 build 48) was used for operating the MS instrument.

Preparation of chlorine dioxide solutions

A 30 wt% aqueous sulfuric acid solution (7.5 mL) was added dropwise to 17.5 mL of an aqueous sodium chlorite solution (300 g/L) in a 100 mL multi-necked flask at an addition rate of 0.5 mL/min at room temperature under a nitrogen flow through the reaction solution. The gaseous chlorine dioxide produced was

introduced with the nitrogen flow into 100 mL of deionized water in another flask pre-cooled at 0 °C along. After sulfuric acid addition was complete, the reaction solution was allowed to remain under nitrogen flushing for another 30 min at room temperature, to give 100 mL of a yellow-colored aqueous solution of chlorine dioxide in the second flask.

The current concentration of chlorine dioxide in the solution was determined by titration. To 1.0 mL of the chlorine dioxide solution, 2.0 mL of a 30 wt% aqueous sulfuric acid solution and 2.0 mL of a 10 wt% aqueous potassium iodide solution were added. The color of the resulting solution turned to dark brown (oxidation of iodide to elemental iodine). The iodine produced was titrated with a 0.1 M sodium thiosulfate solution against starch as the indicator. The concentration according to the above procedure ranged between 50 and 60 mmol/L. The chlorine dioxide solution was diluted with deionized water when necessary (UV measurements).

UV/VIS measurements

A 1 µM solution of DHNQ (2 mL) in water at pH3 (set by sulfuric acid or 0.1 M phosphate buffer) was added into a stirred UV cuvette at 22 °C. Freshly prepared aqueous chlorine dioxide solution (concentration newly determined) was added in amounts corresponding to target DHNQ/ClO_2 molar ratios, the volumes being usually between 0.2 and 2 mL. The visible light absorption of the reaction solution at 550 nm was recorded in 2 s steps.

Degradation of DHNQ by chlorine dioxide

In a 500 mL round-bottom flask, freshly prepared chlorine dioxide solution (concentration newly determined) was added at once to 100 mL of an aqueous DHBQ solution (pH 3, set by sulfuric acid or 0.1 M phosphate buffer), and the mixture was stirred at r.t. in the dark. The amount of chlorine dioxide solution was set in a way that a target DHNQ/ClO_2 molar ratio was reached. At certain time intervals, 5 mL aliquots were taken and extracted twice with 1 mL of $CDCl_3$. The two extracts were combined and analyzed by NMR either directly or after filtration through a pipette (5 cm path) filled with solid $MgSO_4$ or solid $MgSO_4$/K_2CO_3 (w/w = 1:1). Care was taken that the time between taking the aliquot and NMR analysis was less than 30 s (45 s when filtered). The filtered extract was also used for GCMS analysis. In some cases, a drop of *N,O*-bis(trimethylsilyl)-trifluoroacetamide (BSTFA) was added prior to NMR and GCMS runs.

After a reaction time of 2 h, a 50 mL aliquot was analyzed for CO_2 according to standard procedures (precipitation as $BaCO_3$). The remaining solution was extracted and analyzed (GC/MS, NMR) for remaining organic compounds according to a procedure previously optimized for carboxylic acid and hydroxyacids in complex matrices (Liftinger et al. 2015).

1,2,4,5,8-Pentahydroxynaphthalene (intermediate **I**)

^{1}H NMR ($CDCl_3$): δ 6.68 (s, 1H), 6.83 (d, 1H, ^3J = 6.2 Hz), 7.59 (d, 1H, ^3J = 3.1 Hz). 9.3 (s, br, OH). ^{13}C NMR ($CDCl_3$): δ 103.4 (HC-3), 109.6 (C-4a), 116.0 (C-8a), 117.1 (HC-6), 117.9 (HC-7), 138.4 (C-1), 144.2 (C-2), 149.4 (C-8), 150.4 and 150.5 (C-4 and C-5). Analysis as per-trimethylsilylated derivative: ^{1}H NMR ($CDCl_3$): δ 0.30 (s, 27 H, 3 × $SiMe_3$), 0.31 (s, 9 H, 1 × $SiMe_3$), 0.34 (s, 9 H, 1 × $SiMe_3$), 6.72 (s, 1H), 6.81 (d, 1H, ^3J = 6.2 Hz), 7.55 (d, 1H, ^3J = 3.1 Hz). 9.3 (s, br, OH). MS data in main text (Table 1).

Final stable degradation products

Measurement in D_2O/NaOD, pD = 10, assignment confirmed by spiking with authentic samples. CO_{-2}, ^{13}C NMR: δ 170.4. Acetic acid, ^{1}H NMR: δ 1.92; ^{13}C NMR: δ 22.0, 177.9. Glycolic acid, ^{1}H NMR: δ 4.23; ^{13}C NMR: δ 60.6, 177.4. Oxalic acid, ^{13}C NMR: δ 160.4.

Computations

The GAUSSIAN 09 program package was used for all calculations (Frisch et al. 2009). The geometry optimization was carried out at the DFT(M06-2X) level of theory (Zhao et al. 2008). The 6-31G(d) basis sets were employed for H, C, O and Cl, where a diffuse function was added to each of O and a p-polarization function was added to H (these basis sets being named BS-I). It was ascertained that each equilibrium geometry exhibited no imaginary frequency and each transition state exhibited one imaginary frequency.

Enthalpy, entropy, and Gibbs energy changes were evaluated at 298.15 K. Zero-point energy, thermal energy, and entropy change were evaluated at the DFT(M06-2X)/BS-I level. For the water molecule, experimental entropy of water at 298.15 K and 1 atm (16.7 cal/mol K) was employed for the estimation of Gibbs energy.

For single point calculations, either CCSD(T), MP4(SDQ), or DFT(M06-2X) method was employed. The CCDS(T) and MP4(SDQ) methods were mainly employed for the radical and ionic species, respectively. In the CCSD(T) calculations for radicals, restricted open-shell wave functions (ROHF functions) were selected as the reference wave functions, as the unrestricted wave functions (UHF functions) were significantly spin-contaminated. For large species, such as DHNQ-ClO_2 complexes, we employed the DFT(M06-2X) method. In the single point calculations at the CCSD(T) and the DFT(M06-2X) levels, 6-311G(d) basis sets (BS-II) were employed for H, C, O and Cl, where a diffuse function was added to each of O and Cl and a p-polarization function was added to H. For the MP4(SDQ) calculations, we employed other basis sets: the aug-cc-pVTZ basis sets were used for O and Cl and the cc-pVTZ basis sets were selected for C and H, where f-type and d-type functions were omitted from the heavy atoms and hydrogen, respectively, to reduce computational costs (BS-III).

In all calculations, the solvation energy in water was evaluated according to the PCM method. For the determination of the cavity size in the PCM calculations, the UFF parameters and the united atom topological model optimized at the HF/6-31G(d) level of theory were used for geometry optimization and energy evaluation, respectively.

Acknowledgments We performed quantum chemical calculations with the workstation in the Sakaki group, Fukui institute for fundamental chemistry at Kyoto University, Japan, and would like to thank for the access. The financial support of the Austrian Christian Doppler Research Society (CDG) through the CD-lab "Advanced cellulose chemistry and analytics" and the Austrian Research promotion Agency (FFG), project "Chromophores-II", is gratefully acknowledged.

References

Aguilar CAH, Narayanan J, Singh N, Thangarasu P (2014) Kinetics and mechanism for. the oxidation of anilines by ClO_2: a combined experimental and computational study. J Phys Org Chem 27:440–449

Arnone A, Merlini L, Nasini G, Vajna de Pava O (2007) Asymmetric Diels–Alder reactions. Part 6. Regio- and stereo-selective cycloadditions of 5-(2′,3′,4′,6′-tetra-O-acetyl-β-D-glucopyranosyloxy)-1,4-naphthoquinone. Synth Commun 37:2569–2573

Betts RL, Murphy ST, Johnson CR (2004) Enzymatic desymmetrization/resolution of epoxydiols derived from 1,4-naphthoquinone, 5-hydroxy-1,4-naphthoquinone and 5,8-dihydroxy-1,4- naphthoquinone. Tetrahedron Asymmetry 15:2853–2860

Cuellar MA, Salas C, Cortes MJ, Morello A, Maya JD, Preite MD (2003) Synthesis and in vitro trypanocide activity of several polycyclic drimane–quinone derivatives. Bioorg Med Chem 11:2489–2497

Frisch MJ, Trucks GW, Schlegel HB, Scuseria GE, Robb MA, Cheeseman JR, Scalmani G, Barone V, Mennucci B, Petersson GA, Nakatsuji H, Caricato M, Li X, Hratchian HP, Izmaylov AF, Bloino J, Zheng G, Sonnenberg JL, Hada M, Ehara M, Toyota K, Fukuda R, Hasegawa J, Ishida M, Nakajima T, Honda Y, Kitao, O, Nakai H, Vreven T, Montgomery Jr. JA, Peralta JE, Ogliaro F, Bearpark MJ, Heyd J, Brothers EN, Kudin KN, Staroverov VN, Kobayashi R, Normand J, Raghavachari K, Rendell AP, Burant JC, Iyengar SS, Tomasi J, Cossi M, Rega N, Millam NJ, Klene M, Knox JE, Cross JB, Bakken V, Adamo C, Jaramillo J, Gomperts R, Stratmann RE, Yazyev O, Austin AJ, Cammi R, Pomelli C, Ochterski JW, Martin RL, Morokuma K, Zakrzewski VG, Voth GA, Salvador P, Dannenberg JJ, Dapprich S, Daniels AD, Farkas Ö, Foresman JB, Ortiz JV, Cioslowski J, Fox DJ (2009) Gaussian Inc., Wallingford

Greco G, Panzella L, Pezzella A, Napolitano A, d'Ischia M (2010) Reaction of dihydrolipoic acid with juglone and related naphthoquinones: unmasking of a spirocyclic 1,3-dithiane intermediate en route to naphtho[1,4]dithiepines. Tetrahedron 66:3912–3916

Hosoya T, French AD, Rosenau T (2013) Chemistry of 5,8-dihydroxy-[1,4]-naphthoquinone, a key chromophore in aged cellulosics. Mini Rev Org Chem 10(3):309–315

Hull LA, Davis GT, Rosenblatt DH, Williams HKR, Weglein RC (1967) Oxidations of amines. III. Duality of mechanism in the reaction of amines with chlorine dioxide. J Am Chem Soc 89:1163–1170

Kelly TR, Fu Y, Sieglen JT Jr., De Silva H (2000) Synthesis of an orange anthrathiophene pigment isolated from a Japanese bryozoan. Org Lett 2:2351–2352

Korntner P, Hosoya T, Dietz T, Eibinger K, Reiter H, Spitzbart M, Röder T, Borgards A, Kreiner W, Mahler AK, Winter H, French AD, Henniges U, Potthast A, Rosenau T (2015) Chromophores in lignin-free cellulosic materials belong to three compound classes. Chromophores in cellulosics, XII. Cellulose 22(2):1053–1062

Lanari D, Marrocchi A, Minuti L, Taticchi A, Gacs-Baitz E (2002) Synthesis of some new enantiopure [2.2]paracyclophanes bearing polycyclic aromatic subunits. Tetrahedron Asymmetry 13:1331–1335

Lehtimaa T, Kuitunen S, Tarvo V, Vuorinen T (2010) Reactions of aldehydes with chlorous acid and chlorine in dioxide bleaching. Holzforschung 64:555–561

Leigh JK, Rajput J, Richardson DE (2014) Kinetics and mechanism of styrene epoxidation by chlorite: role of chlorine dioxide. Inorg Chem 53:6715–6727

Liftinger E, Zweckmair T, Schild G, Eilenberger G, Böhmdorfer S, Rosenau T, Potthast A (2015) Analysis of degradation products in rayon spinning baths. Holzforschung 69(6):695–702

Mital A, Negi VS, Ramachandran U (2008) Synthesis and biological evaluation of naphthalene-1,4-dione derivatives as potent antimycobacterial agents. Med Chem 4:492–497

Napolitano MJ, Green BJ, Nicoson JS, Margerum DW (2005) Chlorine dioxide oxidations of tyrosine, N-acetyltyrosine, and dopa. Chem Res Toxicol 18:501–508

Potthast A, Schedl A, Zweckmair T, Kikul F, Bacher M, Rosenau T (2018) Pushing the limits: quantification of chromophores in real-world paper samples by GC-ECD and EI-GC-MS. Talanta 179:693–699

Rosenau T, Potthast A, Milacher W, Hofinger A, Kosma P (2004) Isolation and identification of residual chromophores in cellulosic materials. Polymer 45(19):6437–6443

Rosenau T, Potthast A, Kosma P, Suess H-U, Nimmerfroh N (2007) First isolation and identification of residual chromophores from aged bleached pulp samples. Holzforschung 61(6):656–661

Rosenau T, Potthast A, Kosma P, Suess HU, Nimmerfroh N (2008) Chromophores in aged hardwood pulp—their structure and degradation potential. TAPPI J 1:24–30

Schedl A, Korntner P, Zweckmair T, Rosenau T, Potthast A (2016) Detection of cellulose-derived chromophores by ambient ionization-MS. Anal Chem 88:1253–1258

Schedl A, Zweckmair T, Kikul F, Henniges U, Rosenau T, Potthast A (2017) Aging of paper—ultra-fast quantification of 2,5-dihydroxyacetophenone, as a key chromophore in cellulosics, by reactive paper spray-mass spectrometry. Talanta 167:672–680

Tandon VK, Maurya HK (2009) Naphtho [2, 3-b][1, 4]-thiazine-5, 10-diones and 3-substituted-1, 4-dioxo-1, 4-dihydronaphthalen-2-yl-thioalkanoate derivatives: synthesis and biological evaluation. Tetrahedron Lett 50:5896–5902

Tandon VK, Singh RV, Yadav DB (2004) Synthesis and evaluation of novel 1,4-naphthoquinone derivatives as antiviral, antifungal and anticancer agents. Bioorg MedChem Lett 14:2901–2904

Tandon VK, Yadav DB, Chaturvedi AK, Shukla PK (2005a) Synthesis of (1,4)-naphthoquinono-[3,2-c]-1H-pyrazoles and their (1,4)-naphthohydroquinone derivatives as antifungal, antibacterial, and anticancer agents. Bioorg Med Chem Lett 15:3288–3291

Tandon VK, Yadav DB, Singh RV, Chaturvedi AK, Shukla PK (2005b) Synthesis and biological evaluation of novel (L)-alpha-amino acid methyl ester, heteroalkyl, and aryl substituted 1,4-naphthoquinone derivatives as antifungal and antibacterial agents. Bioorg Med Chem Lett 15:5324–5328

Tandon VK, Maurya HK, Verma MK, Kumar R, Shukla PK (2010) 'On water' assisted synthesis and biological evaluation of nitrogen and sulfur containing hetero-1,4-naphthoquinones as potent antifungal and antibacterial agents. Eur J Med Chem 45:2418–2426

Tishchenko O, Truhlar DG, Ceulemans A, Nguyen MT (2008) A unified perspective on the hydrogen atom transfer and proton-coupled electron transfer mechanisms in terms of topographic features of the ground and excited potential energy surfaces as exemplified by the reaction between phenol and radicals. J Am Chem Soc 130:7000–7010

Valderrama JA, Benites J, Cortes M, Pessoa-Mahana H, Prina E, Fournet A (2003) Studies on quinones: part 38. Synthesis and leishmanicidal activity of sesquiterpene 1,4-quinones. Bioorg Med Chem 11:4713–4718

Wenger J, Schedl A, Zweckmair T, Schuhmacher R, Rechthaler J, Herbinger B, Rosenau T, Potthast A (2015) Challenges to detect key-chromophores by paperspray mass spectrometry on cellulosic material. In: Conference proceedings, 18th ISWFPC international symposium on wood, fibre and pulping chemistry, Vienna, Austria, September 09–11, 2015, Vol. II, P121; ISBN: 978-3-900932-24-4

Zhao Y, Truhlar DG (2008) The M06 suite of density functionals for main group thermochemistry, thermochemical kinetics, noncovalent interactions, excited states, and transition elements: two new functionals and systematic testing of four M06-class functionals and 12 other functionals. Theor Chem Acc 120(1–3):215–241

Zhou J, Duan L, Chen H, Ren X, Zhang Z, Zhou F, Liu J, Pei D, Ding K (2009) Atovaquone derivatives as potent cytotoxic and apoptosis inducing agents. Bioorg Med Chem Lett 19:5091–5094

Zwirchmayr NS, Hosoya T, Henniges U, Gille L, Bacher M, Furtmüller P, Rosenau T (2017) Degradation of the cellulosic key chromophore 5,8-dihydroxy-[1,4]-naphthoquinone by hydrogen peroxide under alkaline conditions. J Org Chem 82(21):11558–11565